Results of a New Generation of ITER TF Conductor Samples in SULTAN

P. Bruzzone, B. Stepanov, R. Wesche, E. Salpietro, A. Vostner, K. Okuno, T. Isono, Y. Takahashi, Hyoung Chan Kim, Keeman Kim, A. K. Shikov, and V. E. Sytnikov

***Abstract*—A new generation of ITER TF conductor samples has been assembled and tested in SULTAN in 2007 following a common procedure agreed among the ITER parties. The test results of six SULTAN samples, made of twelve conductor sections manufactured in Europe, Japan, Korea and Russia, are reported here. The conductor layout reflects the ITER TF conductor design, with minor differences for the Nb_3Sn strand characteristics, void fraction and twist pitch. The object of the test is a straight comparison with the ITER requirement of 5.7 K current sharing temperature at 68 kA current and 11.3 T field. A broad range of behavior is observed.**

***Index Terms*—Cable-in-conduit, ITER, Nb_3Sn strand.**

I. Introduction

In 2004, the design of the Cable-in-Conduit conductors (CICC) for ITER was updated [1] by enhancing the j_c specification of the Nb_3Sn strand and increasing the superconductor cross section to offset the performance loss observed in the Model Coils and short samples [2]. In early 2006 two large CICC's made from strands with enhanced J_c were tested in SULTAN with performance below predictions [3]. The first generation of ITER TF prototype conductors has included, beside the nominal "2004-design", minor layout variations aimed to improve the mechanical support of the strands and restrict the transverse load degradation.

Under coordination of the ITER organization (IO), four ITER parties have manufactured twelve short sections of TF conductors, assembled into six twin samples and tested between March and August 2007 in SULTAN. Five out of six samples have been heat treated and assembled at CRPP. The common test program is agreed with IO and includes critical current (I_c) and current sharing temperature (T_{cs}) tests, as well as 1000 load cycles at 68 kA and 11.3 T effective field (10.78 T background field plus self field of the sample).

Manuscript received August 27, 2007. This work was supported by the European Communities under the contract of Association between EURATOM/Swiss, was carried out within the framework of the European Fusion Development Agreement.

P. Bruzzone, B. Stepanov, and R. Wesche are with EPFL-CRPP, Fusion Technology, 5232 Villigen PSI, Switzerland (e-mail: pierluigi.bruzzone@psi.ch; boris.stepanov@psi.ch; rainer.wesche@psi.ch).

E. Salpietro and A. Vostner are with EFDA, Close Support Unit Garching, 85748 Garching b. München, Germany (e-mail: ettore.salpietro@tech.efda.org; alexander.vostner@tech.efda.org).

K. Okuno, T. Isono, and Y. Takahashi are with JAEA, Ibaraki-ken 311-01, Japan (e-mail: okuno.kiyoshi@jaea.go.jp; isono.takaaki@jaea.go.jp).

H. C. Kim and K. Kim are with NFRC, Daejeon 305-333, Korea (e-mail: chankim@nfrc.re.kr; kkeeman@nfrc.re.kr).

A. K. Shikov is with Bochvar Institute, 5 Rogova st., 123060, Moscow, Russian Federation (e-mail: nviinm.400@g23.relcom.ru).

V. E. Sytnikov is with VNIIKP, 111112 Moscow, Russian Federation (e-mail: vsytn@podolsk.ru).

Digital Object Identifier 10.1109/TASC.2008.922266

II. Samples and Conductors Layout

The bare conductor sections, as received at CRPP, are first straightened and cut to the proper length, 3425 mm. The outer diameter is swaged to 42.7 mm in the termination region (except for conductors with diameter <42.7 mm, see Table I and crimping rings are applied to prevent cable-to-jacket slippage during the sample assembly [4]. Short conductor sections are set aside for void fraction measurements.

The heat treatment is carried out in the CRPP vacuum furnace with purge Ar gas flowing inside the conductor. The conductor sections are not constrained in the furnace. Upon heat treatment, 880 ppm elongation is observed on RFTF1 sample (strands by Bochvar Institute, cabling and jacketing by VNIIKP [5]). Strand samples (witness barrels) are also included in the furnace. The heat treatment schedule specified by the conductor suppliers has been applied to each sample.

After heat treatment the jacket is dismantled at both ends and the wraps are stripped from the cable surface. The Cr plating is removed from the strand by dipping the cable in a HCl solution in an ultrasound bath. The cable surface is pre-tinned and eventually soldered into the pre-fabricated Cu-steel upper termination boxes [4]. The lower joint is assembled by soldering the pre-tinned cables to segmented Cu profiles. The joint is then encased into a fully welded steel box, which also acts as mixing chamber for the coolant. The central channel of the CICC is plugged by a 1.5 m long steel rod which extends into the high field region to force the flow in the strand bundle and restrict the temperature and mass flow rate gradients over the cable cross section, see Fig. 1.

The instrumentation attached to the samples consists of voltage taps and temperature sensors. Mass flow rate and pressure sensors, not shown in Fig. 1, are part of the test facility. The T7 and T8 sensors, not foreseen in the original scheme, have only been installed in KOTF and RFTF1 samples. For the main test, the taps V3V9 and V4V10, spanning 450 mm high field section, and the downstream temperature sensors T5 and T6 are retained. In operation, the electromagnetic forces push the cable against the jacket on the side of the voltage taps (outward), see Fig. 1.

The good reliability of the temperature sensors (applied with an advanced procedure) and the high resolution of the data acquisition (down to 1 mK) allow an alternative assessment of T_{cs} by steady state gas flow calorimetry, based on the power criterion: at 68 kA and a 450 mm long high field section, the power threshold is $306\ \mathrm{mW} \equiv 10\ \mu\mathrm{V/m}$.

TABLE I
CONDUCTOR DATA—RESULTS WITH * ARE MEASURED AT CRPP

Sample Nickname	TFPRO1		TFPRO2		JATF2		KOTF		JATF1		RFTF1	
Conductor Nickname	EAS1	EAS2	OST2	OST1	JAB2	JAI2	KO16	KO19	JAI1	JAB1	RF33	RF30
Strand type	Bronze		Internal Sn		Bronze	Int. Sn	Internal Sn		Int. Sn	Bronze	Internal Sn	
Strand identity	NSTT8305		7878	7567, 7603 7730	He2539	6005-K	KAT RC 38c6b7A		6005-K	He2539	BrP	
Strand diameter, mm	0.813		0.815	0.815	0.826	0.820	0.82		0.820	0.826	0.82	
Strand twist pitch, mm	17		17	15	15	10	15		10	15	15	
Cu:non-Cu in strand	0.915		1	1	1	1	0.97		1	1	1	
Cu wire in basic triplet, mm	0.82		0.81	0.82	0.824		0.82		0.824		0.82	
Cable pattern	(2s/c + 1Cu) x 3 x 5 x 5 + core x 6											
Central spiral, mm	6.9 / 9.0		7.0 x 9.1		6.7 x9.0		7 x 9		6.7 x9.0		7 x 9	
Copper cores	3 x 4											
Cu wire in cores, mm	0.81		0.81		0.824		0.82		0.824		0.82	
Pitches of lower stages, mm	45 / 87 / 126 / 245		116/182/ 245/415	45/87/ 126/245	45 / 85 / 130 / 250		41 / 80 / 125 / 240		45 / 85 / 130 / 250		45 / 84 / 124 / 250	
Final cable pitch, mm	486*	492*	520*	520*	447*	454*	820*	508*	450	450	453	
Strand I_c @12T, 4.2K, A	193.3*		265.4*	302.3*	247.2*	281.9*	234.0*		> 248	239	245.9*	
Strand n - index	39.6*		32.0*	23.6*	32.7*	33.7*	29.7*		n.a.	30.1	36.2*	
Av. bundle void fraction, %	33.8*	29.3*	27.7*	29.1*	29.6*	29.8*	34.6*	31.7*	33.5	32.9	32.9*	31.8*
Outer diameter, mm	43.45	42.05	41.45	42.05	42.68	42.66	43.7	43.7	43.9	43.9	43.7	43.7
Cos θ	0.970*	0.971*	0.977*	0.968*	0.967*	0.963*	0.968*	0.970*	n.a.	n.a.	0.967*	0.972*

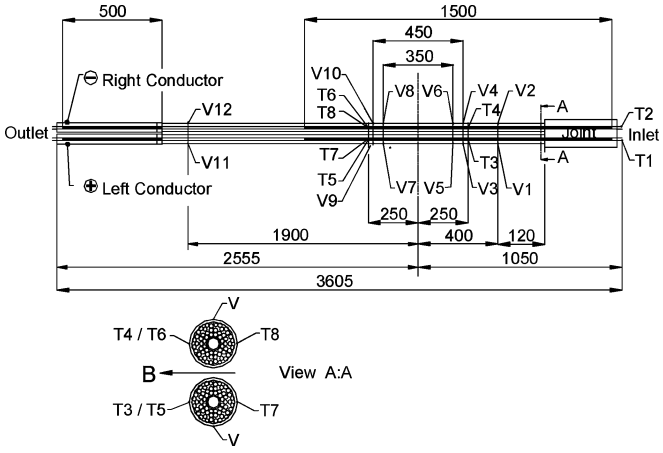

Fig. 1. Standard instrumentation of the SULTAN samples.

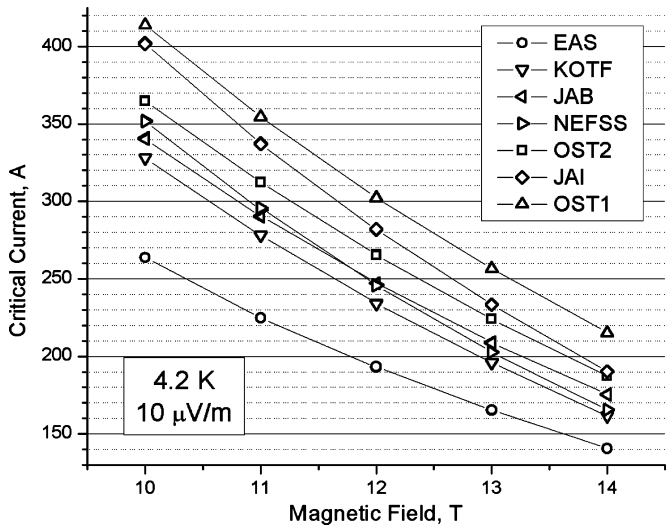

Fig. 2. Summary of I_c vs. magnetic field results for the strand witness samples.

The two conductors of each sample are not identical, see Table I (other data on the conductors are in [4]–[7]). The local void fraction is varied by either reducing the outer diameter (in TFPRO1 from 43.5 mm to 42.0 mm) or using different jacket thickness (in KOTF 1.6 mm and 1.9 mm) or applying more wraps (RFTF1). The JATF1 and JATF2 use the same cables, one JAB and one JAI leg, reduced to lower void fraction in the JATF2, assembled at CRPP. The JATF1 sample is assembled at Toshiba. The OST2 conductor of TFPRO2 use longer twist pitches in the lower cable stages.

The witness strand samples have been tested at liquid helium, variable field. The I_c results of the seven strands are gathered in Fig. 2. Each point in the plot is the average of two test runs of at least two specimens.

III. TEST RESULTS

A. Joint Resistance

For the five samples assembled at CRPP, the joint result has little scattering, see Table II. Larger variation is observed for the connection to the superconducting transformer, which are demountable pressure contacts with an interleaved indium foil. The lowest termination resistance is achieved for JATF1, where indium wires instead of indium foil are used.

On a separate experiment [8], the strand-to-strand resistance within a full size Nb_3Sn termination is measured to be in the range of 10 $n\Omega$. Such low level of resistance ensures a smooth current re-distribution at the joint. For example, a strand with an initial current overload of 30%, i.e. carrying 100 A instead of 75 A in operation, will fully re-distribute the excess current when a voltage as low as 0.25 μV (i.e. 0.5 $\mu V/m$) appears at the high field section of SULTAN.

B. Baseline Voltage

The accuracy of the voltage read-out, after smoothing the noise, is of the order of 200 nV, i.e. about 0.5 $\mu V/m$ for the

TABLE II
SUMMARY OF TEST RESULTS IN SULTAN—BACKGROUND FIELD 10.78 T, EFFECTIVE FIELD 11.3 T @ 68 kA

Sample Nickname	TFPRO1		TFPRO2		JATF2		KOTF		JATF1		RFTF1	
Conductor nickname	EAS1	EAS2	OST2	OST1	JAB2	JAI2	KO16	KO19	JAI1	JAB1	RF33	RF30
Joint Resistance at 0 T, nΩ	0.5		0.5		0.6		0.8		0.6		0.5	
Termination Resistance, nΩ	7.0	5.0	7.5	3.5	1.0	1.2	1.8	1.1	0.5	0.5	2.0	1.4
E Field at 68 kA, 4.5 K, μV/m	2.2	-0.8	-1.1	8.8	7.0	4.4	-25	0.6	2.1	-0.4	-3.0	28.1
E Field at 20 kA, 4.5 K, μV/m	0.4	-0.2	-0.3	2.0	1.7	1.7	-10	0.0	-0.5	-0.5	-1.1	11.1
T_{cs} from raw voltage data, K	5.95	6.32	7.39	5.38	4.58	5.31	6.53	5.67	5.61	6.24	6.16	< 4.5
m index according to (2), -	23.4	12.1	52.4	13.6	11.1	13.1	8.6	11.8	16.5	19.5	13.9	19.0
Est. T_{cs} according to (2), K	**6.35**	**6.35**	**7.35**	**6.50**	**6.40**	**5.95**	**5.45**	**5.80**	**5.50**	**6.40**	**5.90**	**6.25**

voltage taps spaced by 450 mm. Further smoothing may achieve higher resolution only on short time windows.

During a $T_{\rm cs}$ test run, the current is first raised to 68 kA and then the operating temperature is slowly raised from 4.5 K. At the end of the current ramp, the voltage at high field is expected to be 0, i.e. flat baseline voltage. Small deviations from 0, in the range of $\pm 1\ \mu$V ($\pm 2\ \mu$V/m) have little impact on the assessment of $T_{\rm cs}$ and can be neglected as far as the slope of the $V(\mathrm{T})$ curve is $> 20\ \mu$V/K at 4.5 μV (10 μV/m).

In Table II, the results of the voltage baseline are reported for the first run of all the conductors at the end of the current ramp (68 kA) and at an intermediate hold of the current, at 20 kA (for accuracy, see above). Six out of 12 conductors show at the end of the ramp a low voltage level, in the range of 2 μV/m or less. Large voltage is observed on six conductors: negative on RF33 and KO16 and positive on RF30, JAI2, JAB2, OST1. The slope of the $V(\mathrm{I})$ curve is not always constant.

C. Voltage vs. Power Generation

Obviously, a negative voltage sensed at V3V9 or V4V10 taps cannot be a measure of the average longitudinal electric field that is needed for the $T_{\rm cs}$ assessment. The early voltage observed in some of the conductors is due to non-equipotential cable cross section under the voltage taps. These unusually high transverse voltages are linked to local current re-distribution (for re-distribution at the joint, the level of transverse voltage is orders of magnitude lower, see above).

The plot in Fig. 3 shows a $T_{\rm cs}$ run for JAB2 (large positive baseline) and KO16 (large negative baseline). The current ramp is held at various flat tops to read the voltage without inductive components. The power generated at the high field section, P, is measured by gas flow calorimetry at steady state conditions (constant current and temperature profile). The equivalent longitudinal electric field, $E_{\rm cal}$, is deduced from the generated power

$$E_{cal} = \frac{P}{I_{op}\ell} = \frac{\dot{m}(T5 - T3)C_p}{I_{op}\ell} \tag{1}$$

where ℓ is the length of the high field section (450 mm) and $C_{\rm p}$ is the helium specific heat. The temperature increase over the high field section, T5-T3, is measured with the accuracy of ± 2 mK. A comparison of $E_{\rm cal}$ with the readout of the voltage taps confirms that the large "early voltages" do not generate power and should not be retained for a plain assessment of $T_{\rm cs}$.

D. Processing of the Voltage Signals

It is assumed that the same mechanism that produces a transverse voltage at increasing current is also effective at increasing temperature, at least as long as the longitudinal voltage remains much lower than the transverse voltage. Then, a signal processing based on the $V(\mathrm{I})$ signal is appropriate for a $I_{\rm c}$ run, but not for a $T_{\rm cs}$ runs.

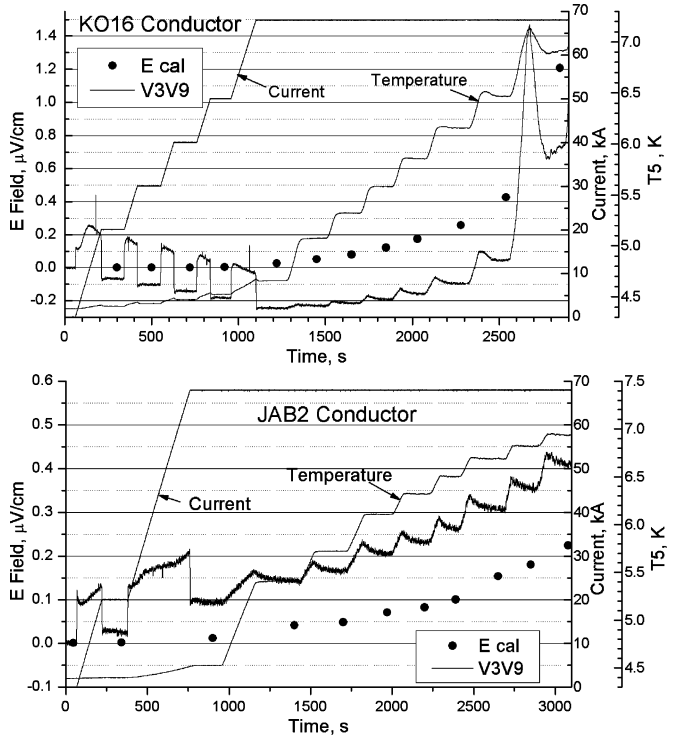

Fig. 3. Comparison of calorimetry and voltage taps in $\mathrm{T_{cs}}$ runs.

As a pragmatic approach to remove the transverse voltage component and extract a $T_{\rm cs}$ figure from the experimental data, we apply a voltage signal processing based on a fitting formula for the $E - T$ curve

$$E(T/T_{cs}) = a \cdot (T/T_{cs}) + E_c(T/T_{cs})^m \tag{2}$$

where $E_{\rm c}$ is the 10 μV/m criterion. The exponent m and the coefficient a are fitting parameters (no physical model behind it). When the baseline voltage is <0, the a parameter turns to be negative. Conceptually, this procedure is similar to a pure power law extrapolation of the $E(\mathrm{T})$ curve from the upper part, where the longitudinal voltage dominates. However, the fit (2) is applicable to lower voltage, far from the large temperature non-homogeneity associated to the thermal runaway.

E. Estimate of T_{cs}

For the conductors with very low voltage at the end of the current ramp, the $T_{\rm cs}$ results numerically obtained from (2), see Table II, are, as expected, very close to the raw data. For EAS2, OST2, KO19 and JAB1, the deviation between raw data and (2) results is within 0.1 K.

When the early voltage is large (positive or negative), the raw data provide much too low or high $T_{\rm cs}$. In these cases, the calorimetric assessment, whose accuracy is eventually limited by the local temperature/mass flow rate gradients in the cable cross section, provides a term of comparison. The deviation between (2) results and calorimetry is only 0.1 K for JAB2.

The m exponent from the fitting formula (2) turns to be very similar for conductors made from the same strand, which is a sign of consistency for the assessment procedure. In OST2, as opposed to all other conductors, the m value, as well as the n index, is same as in the strand.

The performance evolution upon cyclic loading is less pronounced compared to former samples [3]. The fitting procedure partly hides the broadening of the E(T) transition.

The accuracy of the $T_{\rm cs}$ assessment consists of two terms. From the sensors and current meter accuracy, temperature homogeneity and reproducibility, the $T_{\rm cs}$ results are better than ± 0.1 K (this can be directly applied to EAS2, OST2, KO19 and JAB1). The confidence in the voltage processing procedure provides additional uncertainty. The fitting (2) tends to be conservative for conductors with negative baseline $(-0/+0.2\,{\rm K})$ and optimistic $(-0.2\,{\rm K}/+0)$ for conductors with large positive baseline.

IV. Discussion

Comparing Fig. 1 (witness strand) with the $T_{\rm cs}$ results of the CICC, the striking impression is that the ranking of the strand performance has nothing to do with the CICC performance. The strand specification may be even misleading to assess the CICC. For example, the JAI strand has 50% higher j_c @ 12 T, 4.2 K compared to the EAS strand, but the EAS2 conductor has by far better performance than JAI2, although the conductor specification (void fraction and pitches) is identical.

A straight comparison of the impact of the void fraction (33% vs. 30%) shows no difference for the bronze based conductors (EAS1 vs. EAS2 and JAB2 vs. JAB1) and a difference of about 0.4 K for the three internal Sn ones (JAI1 vs. JAI2, KO16 vs. KO19 and RF33 vs. RF30). The reduced void fraction has a visible impact on the ac loss and heat removal from the strand bundle [9].

The large early voltage, dominated by potential differences across the cable, is treated as parasitic signal and is removed for the assessment above. However, such voltages are not observed either in large monolithic $\rm Nb_3Sn$ conductors or in NbTi CICC, and must be considered "abnormal". Evidences from related investigations [10]–[12] suggest that filament breakage from transverse load on the strand bundle may be the reason for local current re-distribution and transverse voltage across the cable.

The broad superconducting transition is a concern for the operation of large coils, where only limited power generation, far below the $T_{\rm cs}$ criterion can be tolerated. The $E(T)$ curve in the range of 1–2 $\mu{\rm V/m}$ cannot be reliably explored for those conductors that show large early voltage.

The issue of qualification of the TF conductor samples for ITER and the impact of the test results on the final conductor layout are discussed in [13].

V. Conclusion

The use of a standardized procedure for sample assembly, instrumentation and test program has been established with satisfactory results as a first step toward a systematic quality control for the large ITER conductors.

For 6 out of 12 conductors, substantial early voltage is observed, preventing a straight assessment of $T_{\rm cs}$ from the raw data. In order to extract a usable $T_{\rm cs}$ figure from those conductors, an ad hoc procedure is suggested to treat the large early voltage. Calorimetric assessments of $T_{\rm cs}$ support the adequacy of the data processing.

The $T_{\rm cs}$ performance of the twelve TF conductors spans from 5.45 K to 7.35 K and does not reflect the $I_{\rm c}$ ranking of the individual strands. A homogenization of the performance toward the upper range is desirable to provide an effective margin for the operation of the ITER TF coil system.

Acknowledgment

The technical support of PSI in the experimental activity is acknowledged. The views and opinions expressed herein do not necessarily reflect those of the European Commission.

References

[1] "ITER Final Design Report," IAEA Vienna and ITER IT team Design Description Document 1.1 Update, Jan. 2004.
[2] N. Mitchell, "Summary, assessment and implications of the ITER model coil test results," *Fusion Eng. Des.*, vol. 66–68, pp. 971–993, 2003.
[3] P. Bruzzone *et al.*, "Test results of two ITER TF conductor short samples using high current density $\rm Nb_3Sn$ strands," *IEEE Appl. Supercond.*, vol. 17, pp. 1370–1373, 2007.
[4] P. Bruzzone *et al.*, "Test results of two European ITER TF conductor samples in SULTAN," presented at the MT20 Conference, paper 4I06.
[5] A. Shikov *et al.*, "Development and Results of Testing in SULTAN Facility of a New RF Produced Internal Tin ITER TF Conductor Sample," in these proceedings.
[6] H. C. Kim *et al.*, "Development and SULTAN Test Results of ITER TF Conductor Samples of Korea," in these proceedings.
[7] Y. Takahashi *et al.*, "Performance of Japanese $\rm Nb_3Sn$ Conductors of Toroidal Field Coils for ITER," in these proceedings.
[8] F. Cau *et al.*, "Interstrand Resistance in the Termination of ITER Conductors," in these proceedings.
[9] Presentations at the ITER Conductor Meeting, Villigen-PSI, Jul. 2–3, 2007.
[10] P. Bruzzone, R. Wesche, and B. Stepanov, "The voltage current characteristic (n value) of the cable-in-conduit conductors for fusion," *IEEE Appl. Supercond.*, vol. 13, pp. 1452–1455, 2003.
[11] Y. Ilyin *et al.*, "Performance of ITER $\rm Nb_3Sn$ Strands Under Spatial Periodic Bending in TARSIS," in these proceedings.
[12] M. C. Jewell, P. J. Lee, and D. C. Larbalestier, "$\rm Nb_3Sn$ Filament Breakage Under Bending Strain at 77 K," in these proceedings.
[13] D. Bessette and N. Mitchell, "Review of the ITER Toroidal Field Conductor R&D and Qualification," in these proceedings.